Journal of Hydrology 677 (2026) 135922

Contents lists available at ScienceDirect

Journal of Hydrology

journal homepage: www.elsevier.com/locate/jhydrol

# A general two-dimensional analytical solution for solute transport in anisotropic porous media with time-varying velocity field, different contaminant sources, and initial contamination

Luigi Cimorelli *, Andrea D'Aniello *

*University of Naples Federico II, Department of Civil, Architectural and Environmental Engineering, via Claudio 21, 80125 Napoli, Italy*

ARTICLE INFO

*Keywords:*
Solute transport
Anisotropy
Off-diagonal dispersion
Green's function
Analytical model

ABSTRACT

This study presents a novel two-dimensional analytical solution for solute transport in homogeneous porous media accounting for the effects of anisotropy in presence of adsorption and decay. The solution is derived using Green's function for an infinite domain and extends existing analytical formulations by relaxing several simplifying assumptions commonly adopted in literature. In particular, the proposed analytical solution accounts for the effects of mechanical dispersion along the non-principal direction of groundwater flow as well as for the dependency of the dispersion tensor on the actual groundwater velocity field, without simplifications or convenient orientations of the model domain. The solution is also general as allows to account for: i) bi-directional groundwater velocity field and its variation over time; ii) source terms of different geometries (e.g., point, line, and surface sources) and temporal variability; iii) general initial concentration distributions of the contaminant concentration. The proposed analytical solution is also tested over benchmark problems conceived with a well-known numerical model for flow and transport in porous media (COMSOL Multiphysics®), and the agreement between the two is excellent.

## 1. Introduction

Globally, groundwater resources meet half of the freshwater demand for domestic use and about 25% for irrigation, for a total of trillions cubic meters per year (United Nations, 2022). However, this precious resource is not spread evenly across the globe, and numerous countries are witnessing its depletion and deterioration due to increasing water stress and contamination (Hibbs and Sharp, 2012; Li et al., 2021, and references therein; Osuoha et al., 2023; Sridhar and Parimalarenganayaki, 2024, and references therein; United Nations, 2024; D'Aniello et al., 2026).

Although costly, difficult, and time consuming, groundwater monitoring and remediation is essential to protect and recover such precious water resources. Among the numerous activities involved in the remediation of contaminated aquifers, groundwater and contaminant transport modeling is indeed crucial to predict the fate of contaminants and to plan proper monitoring and remedial actions. Numerical models are often preferred over analytical models because they have less restrictive assumptions on aquifer properties, domain geometry, and on boundary and initial conditions, thus better handling the heterogeneous and complex nature of the subsurface and of groundwater flow (Istok, 1989; Batu, 2006). However, numerical models require a high computational burden, are time consuming, and do not provide an exact solution to the mathematical problem solved, with results generally affected by numerical diffusion (Zheng and Bennett, 1995). On the other hand, analytical solutions are faster, do not need to be solved for the entire model domain, and provide an exact solution to the mathematical problem (Istok, 1989; Batu, 2006). Therefore, analytical solutions can still be appealing, especially when a high number of simulations need to be performed, like in contaminant source identification problems (Moghaddam et al., 2021; Gómez-Hernández and Xu, 2022). However, to be useful and applicable at the field scale, analytical solutions must address a sufficient level of complexity and should not have too many restrictive assumptions.

In the last decades, the scientific community produced a considerably high number of contributions on the topic, providing several analytical solutions addressing a variety of theoretical and practical aspects of solute transport in porous media, like including different boundary and initial conditions, accounting for steady- or unsteady-state groundwater velocity fields, and comprising different transport

* Corresponding authors.
*E-mail addresses:* luigi.cimorelli@unina.it (L. Cimorelli), andrea.daniello@unina.it (A. D'Aniello).

https://doi.org/10.1016/j.jhydrol.2026.135922
Received 23 March 2026; Received in revised form 15 June 2026; Accepted 23 June 2026
Available online 24 June 2026

mechanisms other than advection, such as dispersion, adsorption, and decay. Listing and describing all of them would be a daunting task, and not of much interest here. However, a selection of a few significant contributions is provided hereinafter, based on the dimensionality of the problem solved: 1D analytical solutions (Chrysikopoulos et al., 1990; Yates, 1990, 1992; Basha and El-Habel, 1993; Bosma and van der Zee, 1993; Leij and van Genuchten, 1995; Kangle et al., 1996; Logan, 1996; Liu et al., 1998; Guerrero and Skaggs, 2010; Guerrero et al., 2013; Shen and Reible, 2015), 2D analytical solutions (Batu, 1993; Zhan et al., 2009; Cihan and Tyner, 2011; Yadav et al., 2012; Yadav and Kumar, 2021), and 3D analytical solutions (Goltz and Roberts, 1986; Leij et al., 1991, 1993; Batu, 1996; Sim and Chrysikopoulos, 1999; Yadav et al., 2012). The interested reader might also find useful and informative the collections of one-, two-, and three-dimensional analytical solutions for solute transport in porous media provided by Wexler (1992), Park and Zhan (2001), and Batu (2006). Although each of these solves specific solute transport problems for different combinations of aquifer properties, boundary and initial conditions, transport mechanisms, groundwater velocity fields, and domain dimensions, all the above consider the porous medium to be isotropic, thus neglecting the effects of mechanical dispersion along the non-principal direction of groundwater flow. This is generally done by considering the solution domain oriented along the main groundwater flow direction or by considering groundwater flow oriented along one of the axes of the domain. As a result, the off-diagonal components of the dispersion tensor are set to zero. This represents a significant restrictive assumption that reduces the applicability of the analytical solutions available in literature to real-world problems. Up to now, the study of Rajput & Singh (2021) is the only one available in literature that provides an analytical solution including the effects of the off-diagonal components of the dispersion tensor. Using Laplace transform (Cimorelli et al., 2015), they obtain an analytical solution solving the two-dimensional solute transport problem in a semi-infinite and initially contaminated aquifer accounting for off-diagonal dispersion components, steady-state groundwater velocity field, different contaminant sources, the presence of adsorption and decay, and the effects of heterogeneity on both groundwater velocity and dispersivity. However, in their study, the spatial variability of background contaminant concentration, groundwater velocity, and dispersion components is modeled through specific nondimensional functional expressions, and there is a loose link between the components of the dispersion tensor and groundwater velocities.

In this framework, the aim of the present work is to expand the class of available analytical solutions for solute transport in porous media to better tackle the complex nature of the migration of contaminants in the subsurface, although under controlled and idealized conditions. In particular, the current study presents a novel two-dimensional analytical solution for solute transport in porous media accounting for the effects of anisotropy. The solution is derived using Green's function and includes the following features: infinite domain, homogeneous and anisotropic porous medium, dispersion varying according to the groundwater velocity field, time-varying (i.e., unsteady-state) bi-directional groundwater flow, adsorption, decay, different types of contaminant sources, and the presence of a potential background contaminant concentration. In the remainder of the article, the theoretical setting of the novel analytical solution is given first, followed by the steps required for its derivation. In the results section, the analytical solution is then tested over benchmark problems created with a well-known numerical model for flow and transport in porous media. Finally, the theoretical and practical implications of the proposed analytical solution are discussed.

## 2. Mathematical formulation

### 2.1. General solution

In presence of a bi-directional groundwater velocity field, anisotropy, mechanical dispersion, adsorption, and decay, considering an infinite domain $\in ]-\infty, +\infty[$, $y \in ]-\infty, +\infty[$ and $t \in [0, \infty[$, the two-dimensional solute transport equation reads as follows:

$$-D_{xx}\frac{\partial^2 C}{\partial x^2} - 2D_{xy}\frac{\partial^2 C}{\partial x \partial y} - D_{yy}\frac{\partial^2 C}{\partial y^2} + v_x\frac{\partial C}{\partial x} + v_y\frac{\partial C}{\partial y} + R\frac{\partial C}{\partial t} + R\lambda C = S(x,y,t) \tag{1}$$

where $x$ and $y$ are the reference Cartesian axes, $t$ is the time, $C$ is the solute concentration, $\mathbf{v} = v_x\hat{\boldsymbol{i}} + v_y\hat{\boldsymbol{j}}$ is the vector of the pore water velocity field, $D_{xx}$, $D_{xy}$, $D_{yy}$ are the components of the dispersion tensor, $R = 1 + \frac{\rho_b K_d}{\varphi}$ the retardation factor assuming a linear isotherm describing the adsorption process, with $\varphi$ the effective porosity, $\rho_b$ the porous medium bulk density, $K_d$ the equilibrium distribution coefficient, $\lambda$ is the solute decay constant, and $S$ is the source/sink term. Molecular diffusion is here neglected because its contribution is generally negligible, except at low groundwater velocities (Wexler, 1992).

Considering the following boundary and initial conditions:

$$\lim_{x\to\pm\infty} C(x,y,t) = 0; \lim_{y\to\pm\infty} C(x,y,t) = 0; \lim_{t\to\infty} C(x,y,t) = 0; C(x,y,0) = \gamma(x,y) \tag{2}$$

under the assumption of unsteady groundwater velocity field in time but uniform in space (e.g., typical of seasonal variations of the groundwater velocity field), the velocity components can be described via a dimensionless function of time $f(t)$, and the components of the dispersion tensor become (Batu, 2006):

$$v_x(t) = u_0 f(t) \tag{3a}$$

$$v_y(t) = v_0 f(t) \tag{3b}$$

$$D_{xx} = \frac{\mathrm{a_T}\, v_0^2 + \mathrm{a_L}\, u_0^2}{\sqrt{u_0^2 + v_0^2}} f(t) = D_{x0} f(t) \tag{3c}$$

$$D_{xy} = \frac{(\mathrm{a_L} - \mathrm{a_T})\, u_0 v_0}{\sqrt{u_0^2 + v_0^2}} f(t) = D_{xy0} f(t) \tag{3d}$$

$$D_{yy} = \frac{\mathrm{a_T}\, u_0^2 + \mathrm{a_L}\, v_0^2}{\sqrt{u_0^2 + v_0^2}} f(t) = D_{y0} f(t) \tag{3e}$$

with $\mathrm{a_L}$, $\mathrm{a_T}$ the longitudinal and transverse dispersivity.

Therefore, Eq. (1) becomes:

$$\left(-D_{x0}\frac{\partial^2 C}{\partial x^2} - 2D_{xy0}\frac{\partial^2 C}{\partial x \partial y} - D_{y0}\frac{\partial^2 C}{\partial y^2} + u_0\frac{\partial C}{\partial x} + v_0\frac{\partial C}{\partial y}\right) f(t) + R\frac{\partial C}{\partial t} + R\lambda C = S(x,y,t) \tag{4}$$

To find a suitable analytical solution, Eq. (4) needs to be reduced into a known form. To this end, a functional transformation $C = z(x,y,t)e^{-\lambda t}$ is performed so that the term $R\lambda C$ disappears:

$$\left(-D_{x0}\frac{\partial^2 z}{\partial x^2} - 2D_{xy0}\frac{\partial^2 z}{\partial x \partial y} - D_{y0}\frac{\partial^2 z}{\partial y^2} + u_0\frac{\partial z}{\partial x} + v_0\frac{\partial z}{\partial y}\right) f(t) e^{-\lambda t} + R\frac{\partial z}{\partial t} e^{-\lambda t} = S(x,y,t) \tag{5}$$

with transformed boundary and initial conditions:

$$\lim_{x\to\pm\infty} z(x,y,t) = 0; \lim_{y\to\pm\infty} z(x,y,t) = 0; \lim_{t\to\infty} z(x,y,t) = 0; z(x,y,0) = \gamma(x,y) \tag{6}$$

Then, using the time variable transformation $T = \int_0^t f(\tau)d\tau = F(t)$ (Crank, 1975) to eliminate $f(t)$ from the differential operator and dividing the whole equation by $R$, Eq. (5) becomes:

$$\frac{1}{R}\left(-D_{x0}\frac{\partial^2 z}{\partial x^2}-2D_{xy0}\frac{\partial^2 z}{\partial x\partial y}-D_{y0}\frac{\partial^2 z}{\partial y^2}+u_0\frac{\partial z}{\partial x}+v_0\frac{\partial z}{\partial y}\right)+\frac{\partial z}{\partial T}=\frac{e^{\lambda F^{-1}(T)}S\left(x,y,F^{-1}(T)\right)}{Rf\left(F^{-1}(T)\right)}=\phi(x,y,T) \tag{7}$$

It is worth pointing out that with the Crank transform of the time variable it is required that the function $f(t)$ is non-negative and such that $T=\int_0^\infty f(\tau)d\tau=\infty$ so that the new time variable has the same domain as the original. This condition is satisfied by a broad class of physically meaningful functions, including constant, periodic, and smoothly varying functions commonly used to represent transient groundwater flow conditions.

This ensures that the transformed boundary and initial conditions are the same as the original problem, that is:

$$\lim_{x\to\pm\infty} z(x,y,T)=0;\ \lim_{y\to\pm\infty} z(x,y,T)=0;\ \lim_{T\to\infty} z(x,y,T)=0;\ z(x,y,0)=\gamma(x,y) \tag{8}$$

However, the presence of the second partial derivative makes Eq. (7) more difficult to solve. Therefore, to further reduce the problem complexity, the following space variable transformation is used:

$$\begin{cases}\xi=x\\ \eta=-\dfrac{D_{xy0}}{D_{x_0}}x+y\end{cases} \tag{9}$$

Applying the new space variables defined above, Eq. (7) becomes:

$$-D_\xi\frac{\partial^2 z}{\partial \xi^2}-D_\eta\frac{\partial^2 z}{\partial \eta^2}+v_\xi\frac{\partial z}{\partial \xi}+v_\eta\frac{\partial z}{\partial \eta}+\frac{\partial z}{\partial T}=\phi(\xi,\eta,T) \tag{10}$$

where the parameters appearing in the equation are defined as:

$$D_\xi=\frac{D_{x0}}{R};D_\eta=\frac{1}{R}\left(D_{y0}-\frac{D_{xy0}^2}{D_{x_0}}\right);v_\xi=\frac{u_0}{R};v_\eta=\frac{1}{R}\left(v_0-u_0\frac{D_{xy0}}{D_{x_0}}\right) \tag{11}$$

Again, since the new space variables have the same domain as the original one, boundary and initial conditions in the new space variables remain unchanged:

$$\lim_{\xi\to\pm\infty} z(\xi,\eta,T)=0;\ \lim_{\eta\to\pm\infty} z(\xi,\eta,T)=0;\ \lim_{T\to\infty} z(\xi,\eta,T)=0;\ z(\xi,\eta,0)=\gamma(\xi,\eta) \tag{12}$$

Eq. (10) is now the canonical form of the advection–dispersion equation. To solve this equation, the Green's function method (Xu et al., 2007) is here used. With a slight abuse of notation, the Green's function $G(\xi,\eta,T|\xi_0,\eta_0,T_0)$ can be introduced directly into the differential operator and equated to the impulsive source term $\delta(\xi-\xi_0)\delta(\eta-\eta_0)\delta(T-T_0)$. This is justified because, although the Green's function of a non–self–adjoint operator should rigorously satisfy the adjoint equation $\mathscr{L}^*[G]=\delta$, in advection–dispersion problems the adjoint operator differs from the original one only by a reversal of the advective terms and of the time axis. As a consequence, the Green's function $G^*(\xi,\eta,T|\xi_0,\eta_0,T_0)$ of $\mathscr{L}$ and that of $\mathscr{L}^*$ $G(\xi,\eta,T|\xi_0,\eta_0,T_0)$ are related by a simple exchange of variables (and a reversal of the time direction):

$$G^*(\xi,\eta,T|\xi_0,\eta_0,T_0)=G(\xi_0,\eta_0,T_0|\xi,\eta,T) \tag{13}$$

and the same analytical expression can be used in practice when constructing the fundamental solution (Appendix A). With that been said, Eq. (10) becomes:

$$-D_\xi\frac{\partial^2 G}{\partial \xi^2}-D_\eta\frac{\partial^2 G}{\partial \eta^2}+v_\xi\frac{\partial G}{\partial \xi}+v_\eta\frac{\partial G}{\partial \eta}+\frac{\partial G}{\partial T}=\delta(\xi-\xi_0)\delta(\eta-\eta_0)\delta(T-T_0) \tag{14}$$

with boundary conditions (Appendix A):

$$\lim_{\xi\to\pm\infty} G(\xi,\eta,T)=0;\ \lim_{\eta\to\pm\infty} G(\xi,\eta,T)=0;\ \lim_{T\to\infty} G(\xi,\eta,T)=0 \tag{15}$$

Therefore, the general solution for $C$ in terms of the Green's function is given by Eq. (16):

$$C(\xi,\eta,T)=e^{-\lambda F^{-1}(T)}\int_0^{+\infty}\int_{-\infty}^{+\infty}\int_{-\infty}^{\infty}\phi(\xi_0,\eta_0,T_0)G(\xi,\eta,T|\xi_0,\eta_0,T_0)d\xi_0 d\eta_0 dT_0+e^{-\lambda F^{-1}(T)}\int_{-\infty}^{+\infty}\int_{-\infty}^{\infty}z(\xi_0,\eta_0,0)G(\xi,\eta,T|\xi_0,\eta_0,0)d\xi_0 d\eta_0 \tag{16}$$

where $z(\xi,\eta,0)=C(\xi,\eta,0)$ is the initial distribution of the contaminant concentration in the transformed space variables.

In order to find $G$, the product solutions method (Xu, et al. 2007) is used:

$$G(\xi,\eta,T|\xi_0,\eta_0,T_0)=X(\xi,T|\xi_0,T_0)Y(\eta,T|\eta_0,T_0) \tag{17}$$

leading to:

$$\left(-D_\xi\frac{\partial^2 X}{\partial \xi^2}+v_\xi\frac{\partial X}{\partial \xi}+\frac{\partial X}{\partial T}\right)Y+\left(-D_\eta\frac{\partial^2 Y}{\partial \eta^2}+v_\eta\frac{\partial Y}{\partial \eta}+\frac{\partial Y}{\partial T}\right)X=\delta(\xi-\xi_0)\delta(\eta-\eta_0)\delta(T-T_0) \tag{18}$$

Due to the right-hand side of Eq. (18), it is not possible to separate the variables. However, with the additional time variable change $T'=T-T_0$, which is a simple time translation, Eq. (18) is transformed into a homogeneous equation for $T'>0$:

$$\left(-D_\xi\frac{\partial^2 X}{\partial \xi^2}+v_\xi\frac{\partial X}{\partial \xi}+\frac{\partial X}{\partial T'}\right)Y+\left(-D_\eta\frac{\partial^2 Y}{\partial \eta^2}+v_\eta\frac{\partial Y}{\partial \eta}+\frac{\partial Y}{\partial T'}\right)X=0 \tag{19}$$

with initial condition:

$$X(\xi|\xi_0,0)Y(\eta|\eta_0,0)=\delta(\xi-\xi_0)\delta(\eta-\eta_0) \tag{20}$$

that allows to separate the variables completely, Eq. (21):

$$X(\xi|\xi_0,0)=\delta(\xi-\xi_0);\ Y(\eta|\eta_0,0)=\delta(\eta-\eta_0) \tag{21}$$

Since Eq. (19) must be identically null, then:

$$-D_\xi\frac{\partial^2 X}{\partial \xi^2}+v_\xi\frac{\partial X}{\partial \xi}+\frac{\partial X}{\partial T'}=0 \tag{22a}$$

$$-D_\eta\frac{\partial^2 Y}{\partial \eta^2}+v_\eta\frac{\partial Y}{\partial \eta}+\frac{\partial Y}{\partial T'}=0 \tag{22b}$$

Therefore, the problem is reduced to two one-dimensional advection–dispersion problems with initial conditions given by Eq. (21) and boundary conditions as follows:

$$\lim_{\xi\to\pm\infty} X(\xi,|\xi_0,T')=0;\ \lim_{\eta\to\pm\infty} Y(\eta,|\eta_0,T')=0 \tag{23}$$

whose solutions (in the time variable $T$) are given by (Appendix B):

$$X(\xi,T|\xi_0,T_0)=\frac{H(T-T_0)}{\sqrt{4\pi D_\xi(T-T_0)}}e^{-\frac{\left[(\xi-\xi_0)-v_\xi(T-T_0)\right]^2}{4D_\xi(T-T_0)}} \tag{24a}$$

$$Y(\eta,T|\eta_0,T_0)=\frac{H(T-T_0)}{\sqrt{4\pi D_\eta(T-T_0)}}e^{-\frac{\left[(\eta-\eta_0)-v_\eta(T-T_0)\right]^2}{4D_\eta(T-T_0)}} \tag{24b}$$

where $H(T-T_0)$ is the Heaviside distribution translated by $T_0$. This is necessary by virtue of the causality of the physical systems and of Green's function, as the response of the system cannot anticipate the input.

Finally, the desired Green's function is given by:

$$G(\xi,\eta,T|\xi_0,\eta_0,T_0) = \frac{H(T-T_0)}{4\pi(T-T_0)\sqrt{D_\xi D_\eta}} e^{-\frac{\left[(\xi-\xi_0)-v_\xi(T-T_0)\right]^2}{4D_\xi(T-T_0)}-\frac{[(\eta-\eta_0)-v_\eta(T-T_0)]^2}{4D_\eta(T-T_0)}} \tag{25}$$

With Eqs. (16) and (25), the solution is given for any source term and any initial concentration in the space variables ($\xi$,$\eta$,$T$), and it can be used directly as it is after conversion to the original variables, Eq. (9). It is also important to notice that if $f(t) = 1$, then the identity $t = T$ holds true, and Eqs. (16) and (25) provide the analytical solution for a steady-state velocity field.

To show how to use the general solution here described, the solutions for a time-constant point source term with no initial contaminant concentration (sec. 2.2.) and for an initial concentration with no source term (sec. 2.3.) are provided hereinafter.

### 2.2. Solution for time-constant point source term with zero initial concentration

Assuming a constant point source of contaminant injected at $x = x_0$ and $y = y_0$ starting at time $t = 0$, the source term can be expressed as $S = \delta(x-x_0)\delta(y-y_0)H(t)S_0$, with $S_0$ a constant contaminant flux, and transformed to:

$$\phi(\xi,\eta,T) = \frac{e^{\lambda F^{-1}(T)}\delta(\xi-\alpha)\delta(\eta-\beta)H\left(F^{-1}(T)\right)S_0}{Rf\left(F^{-1}(T)\right)} = \delta(\xi-\alpha)\delta(\eta-\beta)\phi_0(T) \tag{26}$$

where $\alpha = x_0$ and $\beta = -\frac{D_{xy0}}{D_{x0}}x_0 + y_0$ are the $x_0$ and $y_0$ in the $\xi$, $\eta$ coordinate system. Applying Eq. (16) with initial conditions $C(x,y,0) = 0$, and considering that $t = 0 => T = 0 => \tau = 0 => T_0 = 0$, the solution for time-constant point source term with zero initial concentration, in presence of a bi-directional unsteady velocity field, anisotropy, mechanical dispersion, adsorption, and decay, can be expressed as follows:

$$\begin{aligned} C(\xi,\eta,T) &= e^{-\lambda F^{-1}(T)} \int_0^T \int_{-\infty}^{\infty} \int_{-\infty}^{\infty} \frac{\delta(\xi_0-\alpha)\delta(\eta_0-\beta)\phi_0(\tau)}{4\pi(T-\tau)\sqrt{D_\xi D_\eta}} \\ &\quad e^{-\frac{\left[(\xi-\xi_0)-v_\xi(T-\tau)\right]^2}{4D_\xi(T-\tau)}-\frac{[(\eta-\eta_0)-v_\eta(T-\tau)]^2}{4D_\eta(T-\tau)}} d\xi_0 d\eta_0 d\tau \\ &= e^{-\lambda F^{-1}(T)} \int_0^T \frac{\phi_0(\tau)}{4\pi(T-\tau)\sqrt{D_\xi D_\eta}} e^{-\frac{\left[(\xi-\alpha)-v_\xi(T-\tau)\right]^2}{4D_\xi(T-\tau)}-\frac{[(\eta-\beta)-v_\eta(T-\tau)]^2}{4D_\eta(T-\tau)}} \\ &\quad d\tau = e^{-\lambda F^{-1}(T)} \int_0^T \frac{e^{\lambda F^{-1}(\tau)}S_0}{Rf\left(F^{-1}(\tau)\right)4\pi(T-\tau)\sqrt{D_\xi D_\eta}} \\ &\quad e^{-\frac{\left[(\xi-\alpha)-v_\xi(T-\tau)\right]^2}{4D_\xi(T-\tau)}-\frac{[(\eta-\beta)-v_\eta(T-\tau)]^2}{4D_\eta(T-\tau)}} d\tau \end{aligned} \tag{27}$$

Returning to the original unscaled time variable t (using $\tau = F(\theta) => d\tau = f(\theta)d\theta$) gives:

$$\begin{aligned} C(\xi,\eta,t) &= e^{-\lambda t} \int_0^t \frac{e^{\lambda\theta}S_0}{R4\pi(F(t)-F(\theta))\sqrt{D_\xi D_\eta}} \\ &\quad e^{-\frac{\left[(\xi-\alpha)-v_\xi(F(t)-F(\theta))\right]^2}{4D_\xi(F(t)-F(\theta))}-\frac{[(\eta-\beta)-v_\eta(F(t)-F(\theta))]^2}{4D_\eta(F(t)-F(\theta))}} d\theta \end{aligned} \tag{28}$$

The integral in Eq. (28) cannot be obtained in closed form, but it can be efficiently evaluated using the Gauss-Legendre quadrature method.

Recalling sec. 2.1., when $f(t) = 1$ the time transformation reduces to $T = t$ and $F(\theta) = \theta$. Introducing the change of variable $t - \theta = \tau$, the solution in presence of a steady velocity field is given by:

$$C(\xi,\eta,t) = \int_0^t \frac{e^{-\lambda\tau}S_0}{R4\pi\tau\sqrt{D_\xi D_\eta}} e^{-\frac{\left[(\xi-\alpha)-v_\xi\tau\right]^2}{4D_\xi\tau}-\frac{[(\eta-\beta)-v_\eta\tau]^2}{4D_\eta\tau}} d\tau. \tag{29}$$

Nevertheless, even in this case the integral should be evaluated numerically using the Gauss-Legendre quadrature method.

### 2.3. Solution for an initial concentration with no source term

Considering no source term in Eq. (1) and an initial spatial distribution of the solute concentration:

$$C(x,y,0) = \gamma(x,y) \tag{30}$$

In Test 3 (sec. 3.), the solute is distributed at $t = 0$ over a circular surface according to a truncated Gaussian distribution:

$$\gamma(x,y) = \begin{cases} e^{-\frac{(x-x_c)^2+(y-y_c)^2}{2\sigma^2}} & \text{if } \sqrt{(x-x_c)^2+(y-y_c)^2} \le r \\ 0 & \text{if } \sqrt{(x-x_c)^2+(y-y_c)^2} > r \end{cases} \tag{31}$$

with $x_c$ and $y_c$ the coordinates of the center of the circular surface where the contaminant is initially present, $r$ the cutoff radius, and $\sigma$ the standard deviation.

Using Eq. (16) without the source term, and expressing the solution directly in the original spatial and temporal variables, substitution of Eq. (31) yields:

$$\begin{aligned} C(x,y,t) &= e^{-\lambda t} \int_{x_c-r}^{x_c+r} \int_{y_c-\sqrt{r^2-(x^*-x_c)^2}}^{y_c+\sqrt{r^2-(x^*-x_c)^2}} \frac{e^{-\frac{(x^*-x_c)^2+\left(y^*-y_c\right)^2}{2\sigma^2}}}{4\pi F(t)\sqrt{D_\xi D_\eta}} \\ &\quad e^{-\frac{\left[(x-x^*)-v_\xi F(t)\right]^2}{4D_\xi F(t)}-\frac{\left[(y-y^*)-\frac{D_{xy}}{D_{xx}}(x-x^*)-v_\eta F(t)\right]^2}{4D_\eta F(t)}} dy^* dx^* \end{aligned} \tag{32}$$

where $x^*$ and $y^*$ are the integration variables.

## 3. Results

Before presenting the benchmark problems, it is useful to clarify the conceptual framework underlying the proposed analytical formulation. The analytical solution developed in this study reproduces solute transport in a homogeneous and anisotropic porous medium, with dispersion varying according to the groundwater velocity field, time-varying (i.e., unsteady-state) bi-directional groundwater flow, adsorption, decay, different types of contaminant sources, and the presence of a potential background contaminant concentration. In particular, the assumption of homogeneous porous medium under spatially uniform groundwater flow, with fixed direction and time-dependent magnitude, can be interpreted as an idealized representation of contaminant transport under controlled or quasi-uniform flow conditions, such as those encountered in laboratory-scale experiments or in intermediate-scale aquifer settings. Within this framework, the model is primarily intended to include the effects of anisotropic dispersion and to provide a physically consistent basis for interpreting solute transport processes in porous media under well-defined conditions.

Finally, the test cases presented hereinafter are intended as representative benchmarks of the general analytical framework. Indeed, due to the linearity of the governing equation and the Green's function formulation, the extension of the proposed solution to more complex source configurations (e.g., line or surface sources, as well as time-dependent inputs) follows directly by superposition.

### 3.1. Description of the benchmark problems

The proposed analytical solution, Eq. (16), is here tested over three benchmark problems (referred to as Test 1, Test 2, and Test 3) solved numerically with the software COMSOL Multiphysics® v. 6.4.0.343 (COMSOL, 2025), which solves Eq. (1) by the finite element method. In particular, the Transport of Diluted Species in Porous Media interface of the Subsurface Flow module of COMSOL was used.

The three benchmark problems share the same 2D geometry, namely a square domain of 3048 m x 3048 m oriented along the x- and y-axis, resembling a confined aquifer of finite and constant thickness, in presence of anisotropy and of a bi-directional groundwater velocity field. In Test 1 and in Test 2 the aquifer is initially pristine and is subjected to a point source contaminant flux. In Test 3, the aquifer is initially contaminated and there is no point source contaminant flux (source term). The extension of the domain is sufficiently large to avoid any potential influence on the numerical solution of the boundary conditions along the perimeter of the domain, set to $C = 0$ according to Eq. (2). The numerical mesh consists of 1′314′982 unstructured triangular elements, the maximum time step is set to 0.01 years, and convergence of the numerical solution is ensured by a relative tolerance of 0.001. The first benchmark problem (Test 1) is used to test the proposed analytical solution over a stationary condition (Eq. (29), which represents an extreme condition for Eq. (16), that is steady-state groundwater velocity field and contaminant plume migration (i.e., solute concentration is computed over a considerably long time frame, 100 years, to allow achieving steady-state). Conversely, in the second benchmark problem (Test 2) the groundwater velocity field is allowed to vary over time (Eq. (28) assuming $f(t) = 1 + A\sin\left(\frac{2\pi t}{P}\right)$, with $A = 0.3$ and $P = 0.5\,years$, corresponding to $F(t) = t + \frac{AP}{2\pi}\left[1 - \cos\left(\frac{2\pi t}{P}\right)\right]$, and the contaminant plume migration is evaluated over a time frame of 3 years. It must be pointed out that $f(t)$ remains strictly positive for all times (i.e., $f(t) > 0$), thus avoiding singularities in Eq. (7) and ensuring the validity of the Crank time transformation. The third benchmark problem (Test 3) shares the same features of Test 2 except for the fact that there is no point source contaminant flux, the aquifer is initially contaminated according to Eq. (31), and the contaminant plume migration is evaluated over a time frame of 0.5 years. In all benchmark problems, analytical and numerical solutions are compared along two sections passing through the contaminant source location with a spatial discretization of 0.5 m. The first section, here referred to as "longitudinal", is 900 m long and is oriented along the main direction of the groundwater velocity field, whereas the second section, here referred to as "transverse", is 300 m long and is oriented along the direction perpendicular to the main direction of the groundwater velocity field. All parameters used for the benchmark problems are listed in Table 1. Aquifer and contaminant properties are taken from Wexler (1992) and Batu (2006). Regarding the proposed analytical solution, the integrals were evaluated using Gauss–Legendre quadrature with 128 integration points, computations were performed on a standard desktop workstation, with computational times on the order of a few tens of milliseconds, and the solutions were implemented in VB.NET language, using the Mathdotnet library to perform the Gauss-Legendre quadrature.

**Table 1**
Benchmark problems – Parameters.

| Parameter | Unit | Value | Description |
|---|---|---|---|
| $b$ | m | 30.48 | Aquifer thickness |
| $\varphi$ | | 0.25 | Aquifer effective porosity |
| $v$ | m/s | $2.82 \bullet 10^{-5}$ | Pore water velocity |
| $u_0$ | m/s | $1.69 \bullet 10^{-5}$ | Pore water velocity, x-component |
| $v_0$ | m/s | $2.26 \bullet 10^{-5}$ | Pore water velocity, y-component |
| $a_L$ | m | 9.144 | Longitudinal dispersivity |
| $a_T$ | m | 1.829 | Transverse dispersivity |
| $K_d$ | $m^3/kg$ | $2 \bullet 10^{-4}$ | Equilibrium distribution coefficient |
| $\rho_b$ | $kg/m^3$ | 1400 | Solid phase bulk density |
| $\lambda$ | 1/s | $2.2 \bullet 10^{-9}$ | Decay constant |
| $x_C$ | m | 609.6 | Source location, x-coordinate |
| $y_C$ | m | 609.6 | Source location, y-coordinate |
| $C_0$ | $kg/m^3$ | 1 | Source concentration |
| $Q$ | $m^3/s$ | $4.10 \bullet 10^{-4}$ | Discharge rate |
| $S$ | kg/(s•m) | $5.38 \bullet 10^{-5}$ | Source term, $S = \frac{Q \bullet C_0}{\varphi \bullet b}$ |
| $r$ | m | 25 | Cutoff radius, Eq. 31 |
| $\sigma$ | m | 12.5 | Standard deviation, Eq. 31 |

### 3.2. Comparison between analytical and numerical results

The comparison of the results provided by the proposed analytical solution (sec. 2.1.) with those provided by the numerical model (sec. 3.1.) shows excellent agreement between the two for all benchmark problems (Figs. 1-3; Table 2). In all cases, the physics of solute transport in anisotropic porous media in presence of bi-directional groundwater flow, mechanical dispersion, adsorption, and decay is perfectly caught, and it is consistent with the boundary and initial conditions set up for the three benchmark problems (sec. 3.1.).

As expected, in Test 1 (i.e., steady-state groundwater velocity field, continuous point source contaminant flux, and initially pristine aquifer) the steady-state concentration profile along the two reference axes (i.e., longitudinal and transverse, sec. 3.1.) shows the maximum value at the source location and a progressive reduction far from it, with higher concentrations downstream along the main groundwater flow direction and a symmetric distribution along the transverse axis (Fig. 1). Interestingly, a mismatch between the analytical and the numerical solution can be noticed just at the source location. However, this issue is well-documented in literature and does not depend on the proposed analytical solution itself or on the numerical model used. Indeed, the integral in Eq. (29) cannot be obtained in closed form, and it is evaluated using the Gauss-Legendre quadrature method (sec. 2.2.), which is known to produce unreliable results just at the source location and to its close proximity because the denominator is null at the source (Wexler, 1992). Other than this, the match between analytical and numerical solutions is excellent.

In Test 2 (i.e., unsteady-state groundwater velocity field, continuous point source contaminant flux, initially pristine aquifer), the groundwater velocity field is allowed to vary over time (sec. 3.1.) and the concentration profile is shown in Fig. 2 at 0.5, 1, and 3 years. From 0.5 years onwards, the concentration profile appears to be stable and symmetric along the transverse reference axis (sec. 3.1.), whereas on the longitudinal reference axis (sec. 3.1.) the concentration profile remains stable before the source location and partly after it from 0.5 years already, and its progressive increase in the main groundwater flow direction can be tracked over time (Fig. 2). Again, a mismatch between analytical and numerical solutions is evident at the source location, and the same considerations as for Test 1 apply here. A slight mismatch is also evident along the longitudinal reference axis for the solution at 0.5 years at the front of the migrating contaminant plume (Fig. 2). This is not a concern since it is to be attributed to the spatial/temporal discretization of the numerical model (sec. 3.1.) that is not fine enough to perfectly catch the variation of the groundwater velocity field over time and, thus, the respective effects on the migration of the contaminant plume. This mismatch disappears over time (Fig. 2), and the agreement between analytical and numerical solutions is excellent again.

In Test 3 (i.e., unsteady-state groundwater velocity field, no point source contaminant flux, initially contaminated aquifer), the migration of the contaminant plume initially present within the aquifer according to Eq. (31) can be tracked over time by inspecting the concentration profiles depicted in Fig. 3. As there is no contaminant source, the initial contaminant plume gradually fades over time along the two fixed reference axes (i.e., longitudinal and transverse, sec. 3.1.), moving downstream in the main groundwater flow direction. The agreement between analytical and numerical solutions is excellent. Extremely small differences can be noticed at 0.1 years (Fig. 3) and are to be attributed to the natural numerical diffusion present in the numerical model. An additional refinement of the spatial and temporal discretization of the numerical model would completely eliminate any difference.

To quantify the agreement between analytical and numerical results, the Root Mean Square Error (RMSE) and the Nash-Sutcliffe Efficiency

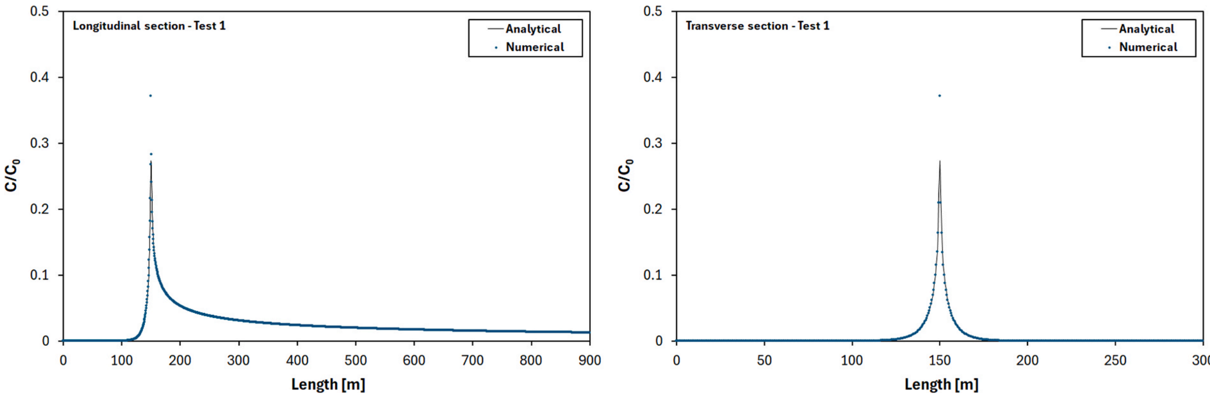


**Fig. 1.** Comparison between analytical and numerical concentration profiles normalized with respect to the concentration at the source along the longitudinal (left) and transverse (right) reference sections for Test 1.

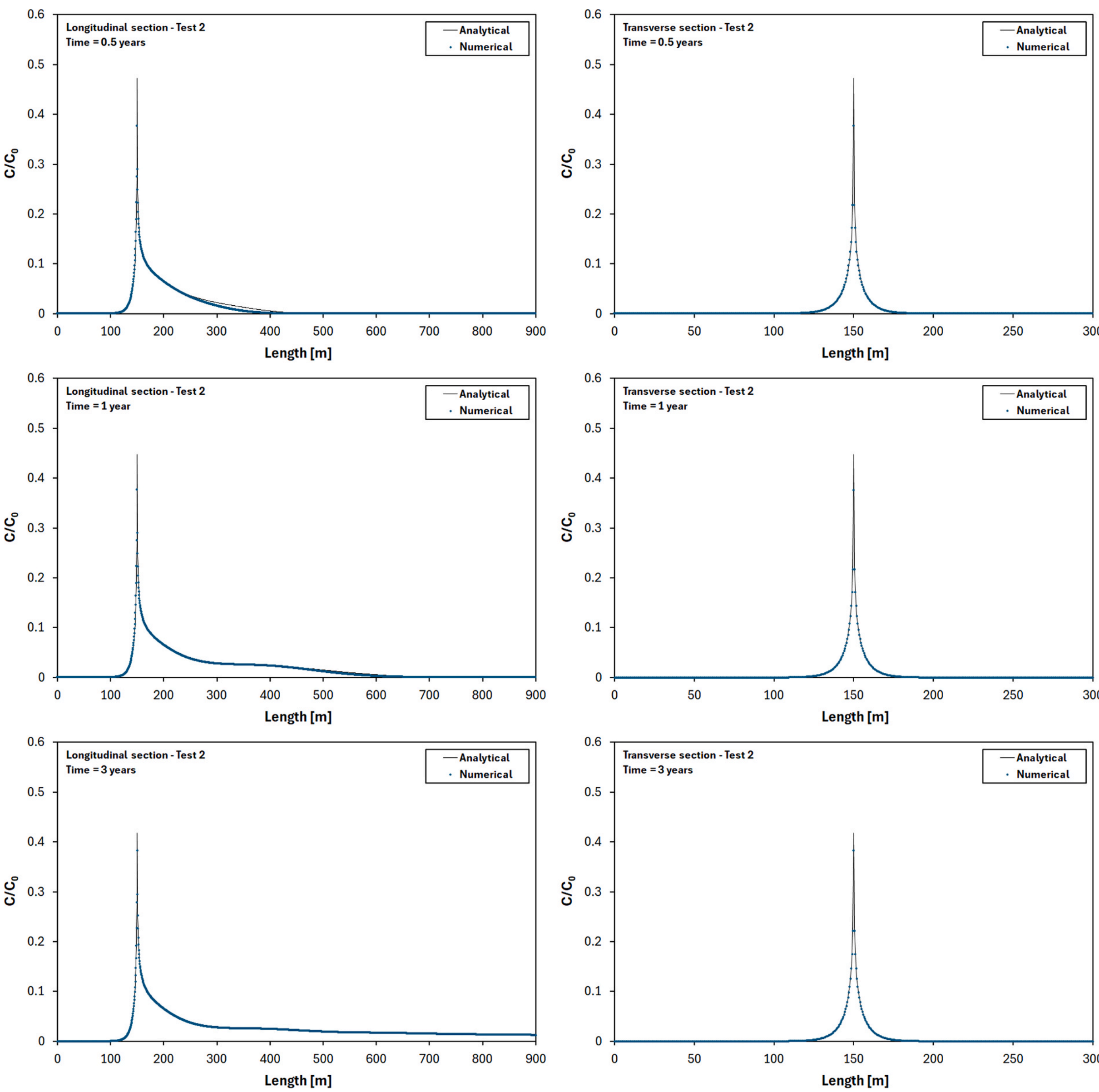


**Fig. 2.** Comparison between analytical and numerical concentration profiles normalized with respect to the concentration at the source along the longitudinal (left panels) and transverse (right panels) reference sections for Test 2 at 0.5, 1, and 3 years. For the sake of brevity, presented time levels are rounded. Actual time levels used for comparison with the numerical model are 0.50484, 1.0048, and 3 years.

**Table 2**
Benchmark problems – Root Mean Square Error (RMSE) and Nash-Sutcliffe Efficiency (NSE) index.

| Test | Time [yr] | RMSE | | NSE | |
|---|---|---|---|---|---|
| | | $C/C_0$ Longitudinal | $C/C_0$ Transverse | $C/C_0$ Longitudinal | $C/C_0$ Transverse |
| 1 | 100 | $2.36 \bullet 10^{-3}$ | $4.08 \bullet 10^{-3}$ | 0.991 | 0.982 |
| 2 | 0.50484 | $3.52 \bullet 10^{-3}$ | $3.95 \bullet 10^{-3}$ | 0.987 | 0.983 |
| | 1.0048 | $2.26 \bullet 10^{-3}$ | $2.96 \bullet 10^{-3}$ | 0.995 | 0.990 |
| | 3 | $8.45 \bullet 10^{-4}$ | $1.51 \bullet 10^{-3}$ | 0.999 | 0.997 |
| 3 | 0.10378 | $3.85 \bullet 10^{-4}$ | $1.84 \bullet 10^{-4}$ | 1.000 | 1.000 |
| | 0.20868 | $2.48 \bullet 10^{-4}$ | $4.39 \bullet 10^{-5}$ | 1.000 | 1.000 |
| | 0.30868 | $2.36 \bullet 10^{-4}$ | $2.17 \bullet 10^{-5}$ | 1.000 | 0.999 |
| | 0.40868 | $1.74 \bullet 10^{-4}$ | $9.30 \bullet 10^{-6}$ | 1.000 | 0.999 |
| | 0.50868 | $1.16 \bullet 10^{-4}$ | $2.88 \bullet 10^{-6}$ | 1.000 | 0.999 |

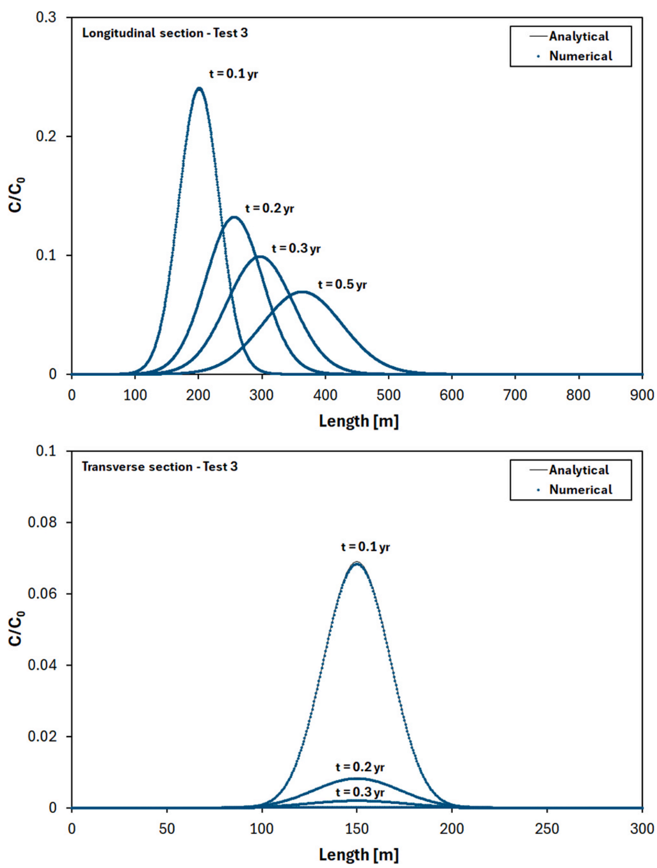


**Fig. 3.** Comparison between analytical and numerical concentration profiles normalized with respect to the maximum concentration of the initial contaminant plume along the longitudinal (top) and transverse (bottom) reference sections for Test 3 at 0.1, 0.2, 0.3, and 0.5 years. For the sake of brevity, presented time levels are rounded. Actual time levels used for comparison with the numerical model are 0.10378, 0.20868, 0.30868, and 0.50868 years.

(NSE) index have been used as indicators:

$$RMSE = \sqrt{\frac{1}{N}\sum_{i=1}^{N}\left[C_a^{(i)} - C_n^{(i)}\right]^2} \quad (33)$$

$$NSE = 1 - \frac{\sum_{i=1}^{N}\left[C_a^{(i)} - C_n^{(i)}\right]^2}{\sum_{i=1}^{N}\left[C_a^{(i)} - \overline{C_a}\right]^2} \quad (34)$$

where $C_a^{(i)}$ and $C_n^{(i)}$ are the solute concentrations computed analytically and numerically at the $i$-th point, respectively, $\overline{C_a}$ is the mean of the solute concentrations computed analytically, and $N$ is the total number of comparison points. Comparisons were performed along the selected profiles using a uniform spatial discretization with a step size of 0.5 m, resulting in 1801 comparison points along the longitudinal reference axis and 601 along the transverse reference axis (sec. 3.1.). Solute concentrations were normalized with respect to the maximum concentration value in each benchmark problem. All points were included in the comparison, including those in the vicinity of the source.

Overall, the excellent agreement between analytical and numerical results is also quantitatively confirmed by the RMSE reaching remarkably low values and by the NSE index approaching unity ($\sim 0.982 - 1$) in the benchmark problems analyzed (Table 2).

## 4. Discussion

### 4.1. Theoretical implications

It should be noted that the spatial transformation adopted in this work, Eq. (9), is not a canonical orthogonal transformation (i.e., not a rotation of the coordinate system), but rather an oblique shear transformation specifically chosen to eliminate the mixed second–order derivative term while preserving the physical and geometrical structure of the problem. Although the problem at hand has been formulated in infinite domain, the proposed transformation is highly suitable for solute transport problems defined in semi–infinite domains with boundary conditions (inflow or zero–flux) applied to one of the coordinate planes. In many groundwater transport applications, the computational domain is semi–infinite and the inflow (or no–flow) boundary condition is imposed on a plane such as $x = 0$. In such cases, it is essential that this boundary remains aligned with one of the axes of the transformed coordinate system. By defining $\xi = x$, the boundary $x = 0$ becomes exactly the boundary $\xi = 0$, and a flow entering orthogonally to the plane $x = 0$ remains orthogonal to the plane $\xi = 0$ after the transformation. This ensures that the physical interpretation of the inflow direction is preserved and that the boundary conditions maintain their original and simple structure.

This property would generally not be maintained under a canonical orthogonal rotation of the coordinate system. A full rotation mixes the coordinates, transforming the original plane $x = 0$ into an oblique line in the rotated system, which in turn complicates the mathematical treatment of the boundary conditions and obscures their physical meaning. By contrast, the shear transformation used here modifies only the direction of the y–axis by redefining $\eta$, while leaving the x–axis (and therefore $\xi$) unchanged. This allows to achieve the desired mathematical simplification (namely, the removal of the mixed derivative term) without modifying the alignment of the boundary plane or the direction of the incoming flow.

It is also worth noting that if the inflow or zero–flux boundary was orthogonal to the y–axis (e.g., on the plane $y = 0$), an equivalent simplification could be obtained by simply rotating the coordinate system by 90° to align that boundary with the x–axis before applying the same shear transformation.

Therefore, although the transformation employed here is not the canonical diagonalization of the dispersion tensor, it remains the most appropriate and physically consistent choice for problems defined in semi–infinite domains with boundary conditions applied on one of the coordinate planes.

### 4.2. Practical implications

To the best of the Authors' knowledge, the proposed analytical solution is the first in literature able to reproduce solute transport in anisotropic porous media in presence of adsorption and decay without a series of restrictive assumptions that make other analytical solutions less general and, so, less applicable. Indeed, the proposed analytical solution includes the effects of mechanical dispersion along the non-principal direction of groundwater flow as well as the dependency of the dispersion tensor on the actual groundwater velocity field (here considered bi-directional and variable over time) and not on specific functions loosely related to it, generally used to simplify the derivation of the analytical solution. Off-diagonal terms in the dispersion tensor represent coupling between orthogonal directions and influence the spreading of the contaminant plume when the principal axes of anisotropy are not aligned with the coordinate system. Therefore, with the proposed analytical solution there is no need to resort to a solution domain oriented along the main groundwater flow direction or to a groundwater flow oriented along one of the axes of the domain to avoid accounting for the presence of the off-diagonal components of the dispersion tensor, as generally done in literature (Wexler, 1992; Park and Zhan, 2001; Batu, 2006). If the groundwater flow field is bi-directional, neglecting the effects of mechanical dispersion along the non-principal groundwater flow direction would result in wider contaminant plumes with lower concentrations in proximity to the source and higher far from it in the transverse direction, whereas, in the longitudinal direction it would result in contaminant plumes of reduced extent with lower concentrations, and, thus, in physically inconsistent predictions of contaminant migration. Furthermore, the analytical solution proposed here is general as it can account for time-dependent variations of the groundwater velocity magnitude through a prescribed scalar function, under the assumption of a spatially uniform groundwater flow field with fixed direction. The same applies to the initial conditions that can be set according to any initial spatial distribution of the contaminant concentration, either as a specific function or as an interpolation of actual field data. In addition, the source term can also be as general as possible, potentially varying over time and according to any geometric entity (point, line, surface) depending on the user needs. Finally, using the principle of superposition, additional variety in terms of source term configuration (i.e., multiple sources) and initial conditions can be easily reproduced.

All these features allow the proposed analytical solution to be used within a range of controlled scenarios, including laboratory-scale experiments and intermediate-scale aquifer settings. For example, it may be used for the calibration of solute transport parameters based on experimental/field evidence, for benchmarking new and existing numerical models, for preliminary assessments of contaminant migration in endangered aquifers, or for contaminant source identification (CSI) problems (Moghaddam et al., 2021; Gómez-Hernández and Xu, 2022), just to name a few. Especially for these last problems, analytical solutions like the one proposed in this work are particularly attractive as inverse problems like CSI can require a tremendous number of simulations that might not be feasible using a numerical model. Indeed, by contrast to numerical models, analytical models are extremely fast (e.g., for the benchmark problems analyzed, it took about 40 ms to compute the analytical solution compared to a maximum of 15 min required by the numerical model with a 13th Gen Intel(R) Core(TM) i7-13700H 2.40 GHz), do not have convergence issues, their results do not depend on the spatial discretization, are not affected by numerical diffusion, and the solution can be computed just where needed, like in observation points where actual measurements are available, without the need to compute the solution over the entire problem domain. Of course, this comes at the expense of model complexity and of the ability to reproduce faithfully real-world scenarios, as simplifying assumptions are necessarily introduced in analytical models. Indeed, the proposed analytical solution is derived for homogeneous porous media and spatially uniform groundwater velocity fields, and it is therefore primarily intended as a tool for analytical investigation rather than for direct field-scale analysis. Future efforts will have to deal with these restrictive assumptions as well. However, as shown in this work, the proposed analytical solution already addresses a series of restrictive assumptions not solved before, moving forward in the direction of expanding the capabilities of analytical models within their traditional domain of applicability.

## 5. Conclusions

In the current study, a novel two-dimensional analytical solution for solute transport in homogeneous porous media accounting for the effects of anisotropy in presence of adsorption and decay is presented. The solution is derived using Green's function and overcomes a series of restrictive assumptions that make existing analytical solutions less applicable. Indeed, the effects of mechanical dispersion along the non-principal direction of groundwater flow as well as the dependency of the dispersion tensor on the actual groundwater velocity field are here explicitly accounted for, without simplifications or convenient orientations of the model domain. The proposed analytical solution is also general, as the groundwater velocity field can be bi-directional and can vary over time through a prescribed scalar function, while maintaining a fixed flow direction. The same applies to the source term that can vary over time and according to any geometric entity (point, line, surface), and to the initial conditions that can be set according to any initial spatial distribution of the contaminant concentration. Although the problem is formulated for an infinite domain, the spatial transformation used to derive the analytical solution is also highly suitable for solute transport problems defined in semi–infinite domains. Within this study, the proposed analytical solution is also tested over benchmark problems conceived with a well-known numerical model for flow and transport in porous media (COMSOL Multiphysics®), and the agreement between the two is excellent.

Overall, the contribution of the present work is primarily methodological, providing an extended analytical framework rather than a direct field scale modeling tool. Nevertheless, the proposed analytical solution is applicable to a variety of controlled settings. For example, it could be used to calibrate solute transport parameters based on experimental/field evidence, to benchmark new and existing numerical models, to make preliminary assessments of contaminant migration in endangered aquifers, or for contaminant source identification problems. Although some limitations still exist, as aquifer heterogeneity and the spatial variability of the groundwater velocity field are not addressed, the proposed analytical solution overcomes a series of assumptions that restricted the applicability of all existing analytical models available in literature until now, allowing to make a step forward in making analytical models more suitable for dealing with real-world problems.

**Funding sources**

This research received no external funding.

**CRediT authorship contribution statement**

**Luigi Cimorelli:** Writing – review & editing, Writing – original draft, Software, Methodology, Investigation, Formal analysis, Conceptualization. **Andrea D'Aniello:** Writing – review & editing, Writing – original draft, Visualization, Validation, Methodology, Investigation, Formal analysis, Conceptualization.

**Declaration of competing interest**

The authors declare that they have no known competing financial interests or personal relationships that could have appeared to influence the work reported in this paper.

## Appendix A

Some abuse of notation was used in sec. 2.1. on the Green's function. Let $L[]$ be the differential operator of the solute transport equation in vectors notation, Ω the domain of z, $\partial\Omega_R$ the generic boundary of Ω with radius R and normal n to its elementary surface element dS. If L is multiplied by the Green's function and integrated over the domain Ω:

$$\int_\Omega G\,L[z]d\Omega = \int_\Omega G\nabla\cdot(-\overline{\overline{D}}\nabla z)d\Omega + \int_\Omega G\mathbf{v}\cdot\nabla z d\Omega + \int_\Omega G\frac{\partial z}{\partial T}d\Omega = \int_\Omega G\phi d\Omega \tag{A.1}$$

Considering the identity $\nabla \bullet (-\overline{\overline{D}}\nabla z\,G) = G\nabla\cdot(-\overline{\overline{D}}\nabla z) - \overline{\overline{D}}\nabla z\cdot\nabla G$ and applying the divergence theorem, the first integral on the right-hand side becomes:

$$\int_\Omega G\nabla\cdot(-\overline{\overline{D}}\nabla z)d\Omega = \int_\Omega \overline{\overline{D}}\nabla z\cdot\nabla G d\Omega - \int_{\partial\Omega_R} G\overline{\overline{D}}\nabla z\cdot\mathbf{n}dS \tag{A.2}$$

Using the identity $\nabla \bullet (z\overline{\overline{D}}\nabla G) = z\nabla \bullet (\overline{\overline{D}}\nabla G) + \overline{\overline{D}}\nabla z \bullet \nabla G$ and applying the divergence theorem again:

$$\int_\Omega G\nabla\cdot(-\overline{\overline{D}}\nabla z)d\Omega = \int_\Omega z\nabla \bullet (-\overline{\overline{D}}\nabla G)d\Omega + \int_{\partial\Omega_R}(z\overline{\overline{D}}\nabla G\cdot\mathbf{n} - G\overline{\overline{D}}\nabla z\cdot\mathbf{n})dS = \int_\Omega z\nabla \bullet (-\overline{\overline{D}}\nabla G)d\Omega \tag{A.3}$$

The last equality holds because both z and G vanish as the radius R goes to infinity. Resorting to the identity $\nabla\cdot(Gz\mathbf{v}) = Gz\nabla\cdot\mathbf{v} + z\mathbf{v}\cdot\nabla G + G\mathbf{v}\cdot\nabla z$, the divergence theorem, and recalling that $\nabla\cdot\mathbf{v} = 0$, the second integral on the right-hand side of Eq. (A.1) becomes:

$$\int_\Omega G\mathbf{v}\cdot\nabla z d\Omega = \int_{\partial\Omega_R} Gz\mathbf{v}\cdot\mathbf{n}dS - \int_\Omega z\mathbf{v}\cdot\nabla G d\Omega = -\int_\Omega z\mathbf{v}\cdot\nabla G d\Omega \tag{A.4}$$

Finally, integrating by parts the last integral of the right-hand side of Eq. (A.1):

$$\int_\Omega G\frac{\partial z}{\partial T}d\Omega = \int_{-\infty}^{+\infty}\int_{-\infty}^{\infty} Gz|_0^\infty d\xi d\eta - \int_\Omega z\frac{\partial G}{\partial T}d\Omega = -\int_{-\infty}^{+\infty}\int_{-\infty}^{\infty} Gz|_{T=0}d\xi d\eta - \int_\Omega z\frac{\partial G}{\partial T}d\Omega \tag{A.5}$$

With the last identity holding because both G and z vanish as T approaches infinity. Putting everything together:

$$\int_\Omega G\,L[z]d\Omega = \int_\Omega z\left[\nabla \bullet (-\overline{\overline{D}}\nabla G) - \mathbf{v}\cdot\nabla G - \frac{\partial G}{\partial T}\right]d\Omega - \int_{-\infty}^{+\infty}\int_{-\infty}^{\infty} Gz|_{T=0}d\xi_0\eta_0 = \int_\Omega G\phi d\Omega \tag{A.6}$$

The term within square brackets is called the adjoint differential operator $L^*$ of L. According to the Green's function, $L^*[G] = \delta(\xi - \xi_0)\delta(\eta - \eta_0)\delta(T - T_0)$, and then:

$$\int_\Omega zL^*[G]d\Omega = \int_\Omega z\delta(\xi - \xi_0)\delta(\eta - \eta_0)\delta(T - T_0)d\Omega = z(\xi_0, \eta_0, T_0) \tag{A.7}$$

As a consequence:

$$z(\xi_0, \eta_0, T_0) = \int_{-\infty}^{+\infty}\int_{-\infty}^{\infty} Gz|_{T=0}d\xi d\eta + \int_0^\infty\int_{-\infty}^{+\infty}\int_{-\infty}^{+\infty} G(\xi_0, \eta_0, T_0|\xi, \eta, T)\phi(\xi, \eta, T)d\xi d\eta dT \tag{A.8}$$

Therefore, the solution is obtained in terms of the variables $\xi_0, \eta_0, T_0$ and the adjoint operator is similar to the original operator but with reversed time axis and reversed velocity vector. By applying $L^*$ to z and by multiplying by the adjoint Green's function $G^*$ and finally integrate over the entire domain Ω:

$$z(\xi, \eta, T) = \int_{-\infty}^{\infty}\int_{-\infty}^{\infty} Gz|_{T_0=0}d\xi_0 d\eta_0 + \int_0^\infty\int_{-\infty}^{\infty}\int_{-\infty}^{\infty} G^*(\xi, \eta, T|\xi_0, \eta_0, T_0)\phi(\xi_0, \eta_0, T_0)d\xi_0 d\eta_0 dT_0 \tag{A.9}$$

Therefore, it can be concluded that $G^*(\xi, \eta, T|\xi_0, \eta_0, T_0) = G(\xi_0, \eta_0, T_0|\xi, \eta, T)$. In sec. 2.1., the adjoint Green's function was used. However, since Eq. (A.9) shows that the Green's function of the adjoint operator coincides with that of the original operator up to an exchange of variables, the distinction between $G$ and $G^*$ becomes immaterial for the present problem. This validates the use of the simplified notation $G$ in the main text.

## Appendix B

The solution of the one-dimensional advection–dispersion equation over an infinite space domain can be found by means of the Fourier Transform with respect to the space variable:

$$\mathscr{F}[X(\xi, T'|\xi_0)] = \int_{-\infty}^{+\infty} X(\xi, T'|\xi_0)e^{-i\omega\xi}d\xi = X(\omega, T') \tag{B.1}$$

Appling the Fourier transform to Eq. (22a) and its initial condition in Eq. (21), and using the properties:

$$\mathscr{F}\left[\frac{\partial X(\xi,T'|\xi_0)}{\partial \xi}\right]=i\omega X(\omega,T');\mathscr{F}\left[\frac{\partial^2 X(\xi,T'|\xi_0)}{\partial \xi^2}\right]=-\omega^2 X(\omega,T') \tag{B.2}$$

one gets Eq. (B.3):

$$\omega^2 D_\xi X(\omega,T')+v_\xi i\omega X(\omega,T')+\frac{\partial X(\omega,T')}{\partial T'}=0$$

$$X(\omega,0)=e^{-i\omega\xi_0} \tag{B.3}$$

Eq. (B.3) has the known solution:

$$X(\omega,T')=e^{-\omega^2 D_\xi T'-i\omega v_\xi T'-i\omega\xi_0} \tag{B.4}$$

To obtain the solution in the $T'$ domain, the inverse Fourier Transform is applied:

$$X(\xi,T'|\xi_0)=\frac{1}{2\pi}\int_{-\infty}^{+\infty}X(\omega,T')e^{i\omega\xi}d\omega=\frac{1}{2\pi}\int_{-\infty}^{+\infty}e^{-\omega^2 D_\xi T'+i\omega\left(\xi-\xi_0-v_\xi T'\right)}d\omega \tag{B.5}$$

using $a=\xi-\xi_0-v_\xi T'$ and applying the complex exponential formula:

$$\frac{1}{2\pi}\int_{-\infty}^{+\infty}e^{-\omega^2 D_\xi T'+i\omega a}d\omega=\frac{1}{2\pi}\int_{-\infty}^{+\infty}e^{-\omega^2 D_\xi T'}\cos(a\omega)d\omega+\frac{i}{2\pi}\int_{-\infty}^{+\infty}e^{-\omega^2 D_\xi T'}\sin(a\omega)d\omega \tag{B.6}$$

The second term on the right-hand side is zero as the integrand is an odd function, while the properties of the even functions can be applied to the first term to give Eq (B.7):

$$X(\xi,T'|\xi_0)=\frac{1}{\pi}\int_0^{+\infty}e^{-\omega^2 D_\xi T'}\cos(a\omega)d\omega=I \tag{B.7}$$

To evaluate this last integral, the Feynman trick is used:

$$\frac{dI}{da}=-\frac{1}{\pi}\int_0^{+\infty}\omega e^{-\omega^2 D_\xi T'}\sin(a\omega)d\omega=\frac{e^{-\omega^2 D_\xi T'}\sin(a\omega)}{2D_\xi T'}\bigg|_0^{\infty}-\frac{a}{2D_\xi T'}\frac{1}{\pi}\int_0^{+\infty}e^{-\omega^2 D_\xi T'}\cos(a\omega)d\omega=-\frac{a}{2D_\xi T'}I \tag{B.8}$$

Therefore:

$$\frac{dI}{da}+\frac{a}{2D_\xi T'}I=0 \tag{B.9}$$

The solution of the first order differential equation is given by:

$$I=I(0)e^{-\frac{a^2}{4D_\xi T'}} \tag{B.10}$$

with $I(0)=\frac{1}{\pi}\int_0^{+\infty}e^{-\omega^2 D_\xi T'}d\omega=\frac{1}{\pi\sqrt{D_\xi T'}}\int_0^{+\infty}e^{-\theta^2}d\theta=\frac{1}{\sqrt{4\pi D_\xi T'}}$.

Finally, substituting into Eq. (B9) and substituting $T'=T-T_0$:

$$X(\xi,T|\xi_0,T_0)=\frac{H(T-T_0)}{\sqrt{4\pi D_\xi(T-T_0)}}e^{-\frac{\left[(\xi-\xi_0)-v_\xi(T-T_0)\right]^2}{4D_\xi(T-T_0)}} \tag{B.11}$$

The same procedure can be applied to derive $Y(\eta,T|\eta_0,T_0)$ from Eq. (22b).

## Data availability

No data was used for the research described in the article.

All data supporting this study are available within the manuscript. The VB.NET scripts of the analytical solutions will be made available on request.

## References

Basha, H.A., El-Habel, F.S., 1993. Analytical solution of the one-dimensional time-dependent transport equation. Water Resour. Res. 29 (9), 3209–3214.

Batu, V., 1993. A generalized two-dimensional analytical solute transport model in bounded media for flux-type finite multiple sources. Water Resour. Res. 29 (8), 2881–2892.

Batu, V., 1996. A generalized three-dimensional analytical solute transport model for multiple rectangular first-type sources. J. Hydrol. 174 (1–2), 57–82.

Batu, V., 2006. Applied flow and solute transport modeling in aquifers: Fundamental principles and analytical and numerical methods. CRC Press.

Bosma, W.J.P., van der Zee, S.E., 1993. Transport of reacting solute in a one-dimensional, chemically heterogeneous porous medium. Water Resour. Res. 29 (1), 117–131.

Cihan, A., Tyner, J.S., 2011. 2-D radial analytical solutions for solute transport in a dual-porosity medium. Water Resour. Res. 47 (4).

COMSOL (2025) Subsurface Flow Module User's Guide – Version 6.4. COMSOL Multiphysics. URL: https://doc.comsol.com (accessed February 5, 2026).

Chrysikopoulos, C.V., Kitanidis, P.K., Roberts, P.V., 1990. Analysis of one-dimensional solute transport through porous media with spatially variable retardation factor. Water Resour. Res. 26 (3), 437–446.

Cimorelli, L., Cozzolino, L., Della Morte, R., Pianese, D., Singh, V.P., 2015. A new frequency domain analytical solution of a cascade of diffusive channels for flood routing. Water Resources Research 51 (4), 2393–2411.

Crank, J., 1975. The mathematics of diffusion. Clarendon-Oxford University Press.

D'Aniello, A., Pirone, D., Cimorelli, L., Pianese, D., 2026. A comparative analysis of different physically based modeling approaches to predict the fate of sewer leaks and their effects on urban aquifer recharge and contamination. J. Hydrol. 667, 134948. https://doi.org/10.1016/j.jhydrol.2026.134948.

Goltz, M.N., Roberts, P.V., 1986. Three-dimensional solutions for solute transport in an infinite medium with mobile and immobile zones. Water Resour. Res. 22 (7), 1139–1148.

Gómez-Hernández, J.J., Xu, T., 2022. Contaminant source identification in aquifers: a critical view. Math. Geosci. 54 (2), 437–458.

Guerrero, J.P., Skaggs, T.H., 2010. Analytical solution for one-dimensional advection–dispersion transport equation with distance-dependent coefficients. J. Hydrol. 390 (1–2), 57–65.

Guerrero, J.P., Pontedeiro, E.M., Van Genuchten, M.T., Skaggs, T.H., 2013. Analytical solutions of the one-dimensional advection–dispersion solute transport equation subject to time-dependent boundary conditions. Chem. Eng. J. 221, 487–491.

Hibbs, B.J., Sharp Jr, J.M., 2012. Hydrogeological impacts of urbanization. Environ. Eng. Geosci. 18 (1), 3–24.

Istok, J.D., 1989. Groundwater modeling by the finite element method. American Geophysical Union, Washington, DC, p. 132.

Kangle, H., van Genuchten, M.T., Renduo, Z., 1996. Exact solutions for one-dimensional transport with asymptotic scale-dependent dispersion. App. Math. Model. 20 (4), 298–308.

Leij, F.J., Skaggs, T.H., van Genuchten, M.T., 1991. Analytical solutions for solute transport in three-dimensional semi-infinite porous media. Water Resour. Res. 27 (10), 2719–2733.

Leij, F.J., Toride, N., van Genuchten, M.T., 1993. Analytical solutions for non-equilibrium solute transport in three-dimensional porous media. J. Hydrol. 151 (2–4), 193–228.

Leij, F.J., van Genuchten, M.T., 1995. Approximate analytical solutions for solute transport in two-layer porous media. Transp. Porous Media 18 (1), 65–85.

Li, P., Karunanidhi, D., Subramani, T., Srinivasamoorthy, K., 2021. Sources and consequences of groundwater contamination. Arch. Environ. Contam. Toxicol. 80 (1), 1–10.

Liu, C., Ball, W.P., Ellis, J.H., 1998. An analytical solution to the one-dimensional solute advection-dispersion equation in multi-layer porous media. Transp. Porous Media 30 (1), 25–43.

Logan, J.D., 1996. Solute transport in porous media with scale-dependent dispersion and periodic boundary conditions. J. Hydrol. 184 (3–4), 261–276.

Moghaddam, M.B., Mazaheri, M., Samani, J.M.V., 2021. Inverse modeling of contaminant transport for pollution source identification in surface and groundwaters: a review. Groundw. Sustain. Dev. 15, 100651.

Osuoha, J.O., Anyanwu, B.O., Ejileugha, C., 2023. Pharmaceuticals and personal care products as emerging contaminants: need for combined treatment strategy. Journal of Hazardous Materials Advances 9, 100206.

Park, E., Zhan, H., 2001. Analytical solutions of contaminant transport from finite one-, two-, and three-dimensional sources in a finite-thickness aquifer. J. Contam. Hydrol. 53 (1–2), 41–61.

Rajput, S., Singh, M.K., 2021. Off-diagonal dispersion effect with pollutant migration in groundwater system. J. Eng. Mech. 147 (12), 04021114.

Shen, X., Reible, D., 2015. An analytical solution for one-dimensional advective–dispersive solute equation in multilayered finite porous media. Transp. Porous Media 107 (3), 657–666.

Sim, Y., Chrysikopoulos, C.V., 1999. Analytical solutions for solute transport in saturated porous media with semi-infinite or finite thickness. Adv. Water Resour. 22 (5), 507–519.

Sridhar, D., Parimalarenganayaki, S., 2024. A comprehensive review on groundwater contamination due to sewer leakage: sources, detection techniques, health impacts, mitigation methods. Water Air Soil Pollut. 235 (1), 56.

United Nations (2022). The United Nations World Water Development Report 2022: Groundwater: Making the invisible visible. UNESCO, Paris. ISBN 978-92-3-100507-7.

United Nations (2024). The United Nations World Water Development Report 2024: Water for Prosperity and Peace. UNESCO, Paris. ISBN 978-92-3-100657-9.

Wexler, E. J. (1992). Analytical solutions for one-, two-, and three-dimensional solute transport in ground-water systems with uniform flow. US Government Printing Office.

Xu, Z., Travis, J.R., & Breitung, W. (2007). Green's function method and its application to verification of diffusion models of GASFLOW code. Forschungszentrum Karlsruhe GmbH, Karlsruhe. Report No. FZKA-7293.

Yadav, R.R., Jaiswal, D.K., Gulrana, 2012a. Two-dimensional solute transport for periodic flow in isotropic porous media: an analytical solution. Hydrol. Process. 26 (22), 3425–3433.

Yadav, R.R., Jaiswal, D.K., Yadav, H.K., Gulrana, 2012b. Three-dimensional temporally dependent dispersion through porous media: analytical solution. Environ. Earth Sci. 65 (3), 849–859.

Yadav, R.R., Kumar, L.K., 2021. Analytical solution of two-dimensional conservative solute transport in a heterogeneous porous medium for varying input point source. Environ. Earth Sci. 80 (8), 327.

Yates, S.R., 1990. An analytical solution for one-dimensional transport in heterogeneous porous media. Water Resour. Res. 26 (10), 2331–2338.

Yates, S.R., 1992. An analytical solution for one-dimensional transport in porous media with an exponential dispersion function. Water Resour. Res. 28 (8), 2149–2154.

Zhan, H., Wen, Z., Huang, G., Sun, D., 2009. Analytical solution of two-dimensional solute transport in an aquifer–aquitard system. J. Contam. Hydrol. 107 (3–4), 162–174.

Zheng, C., Bennett, G.D., 1995. Applied contaminant transport modeling. Theory and Practice, Van Nostrand-Reinhold, New York, USA.